First Scientific Results: Analysis of LIGO Data from the S1 Science Run

Albert Lazzarini
LIGO Laboratory

Annual NSF Review of LIGO Laboratory
17 - 19 November 2003
LIGO Livingston Observatory, LA

LIGO-G030547-06-E

Outline

- Analysis Organization, Tools & Facilities
- Overview of S1 analysis:
  - Burst (Unmodeled transient) Sources
  - Binary Coalescence.
  - Pulsars and CW Sources.
  - Stochastic Background
- Prospects for S2, S3 analyses

Data analysis organization
LIGO Scientific Collaboration (LSC)

- Data analysis is organized in four working groups organized by source type
  Each has two co-chairs:
  - **Binary Inspiral Group**: Patrick Brady [UWM], Gabriela Gonzalez [LSU]
  - **Pulsars/CW Group**: Maria Alessandra Papa [AEI], Mike Landry [LHO]
  - **Stochastic BG Group**: Joe Romano [UTB], Peter Fritschel [MIT]
  - **Burst Group**: Erik Katsavounidis [MIT], Stan Whitcomb [CIT]
  - Leadership represented by astrophysics/phenomenology *and* interferometry/detector expertise
- LIGO S1 author list includes > 300 individuals and ~30 institutions from the USA, Europe, and Asia.
- Scientific oversight of results provided by LSC Executive Committee, and selected panel of internal reviewers from the collaboration.

Data analysis organization

According to source characteristics

- Deterministic signals -- ***Binary coalescences, Periodic sources***
  - »Amplitude and frequency evolution parameterized
  - »Set of templates covering parameter space matched to data
  - » http://www.lsc-group.phys.uwm.edu/pulgroup/
  - » http://www.lsc-group.phys.uwm.edu/iulgroup/
- Statistical signals -- ***Stochastic gravitational wave background***
  - »Cross-correlation of detector pairs, look for correlations above statistical variations
  - » http://feynman.utb.edu/~joe/research/stochastic/upperlimits/
- Unmodeled signals -- ***Supernovae, Gamma Ray Bursts, …***
  - »Non-parametric techniques
    - Excess power in frequency-time domain
    - Excess amplitude change, rise-time in time domain
  - » http://www.ligo.caltech.edu/~ajw/bursts/bursts.html
- *In all cases: coincident observations among multiple detectors*

Data analysis organization
Tools and Facilities

- Data Analysis Tools:
  - » Real-time data QA, post run ancillary channel veto analysis using same tools as used on-line -- Data Monitor Tool (DMT)
  - » Parallel (MPI) analysis with clusters -- LIGO Data Analysis System (LDAS)
  - » Autonomous analysis on clusters -- Condor (batch job manager)
  - » Work-station pos-tprocessing of results
    - – Matlab (graphical/analytical analysis)
    - – ROOT (high energy physics analysis environment)
  - » Software Libraries: LAL, LALAPPS, DMT, Frame, FFTW, LIGOtools, …
- Computational, Archive Facilities
  - » Tier 1 Center: Caltech (210 dual nodes + archive of all level 1 data in SAM-QFS system)
    - – Other LIGO sites: LLO (70 dual nodes), LHO (140 dual nodes), MIT (112 nodes),
  - » Tier 2 Centers: UWM (Medusa, 300 nodes), PSU (141 dual nodes)
  - » Other LSC resources:
    - – US: UTB (Lobizon, 128 nodes)
    - – EU: AEI/Germany(Merlin, 180 dual nodes), Cardiff/UK (80 dual nodes)

Sensitivity during S1

During S1 the 3 LIGO interferometers offered the opportunity for the most sensitive ***coincidence*** observations ever made in the low frequency band around a few hundred Hertz

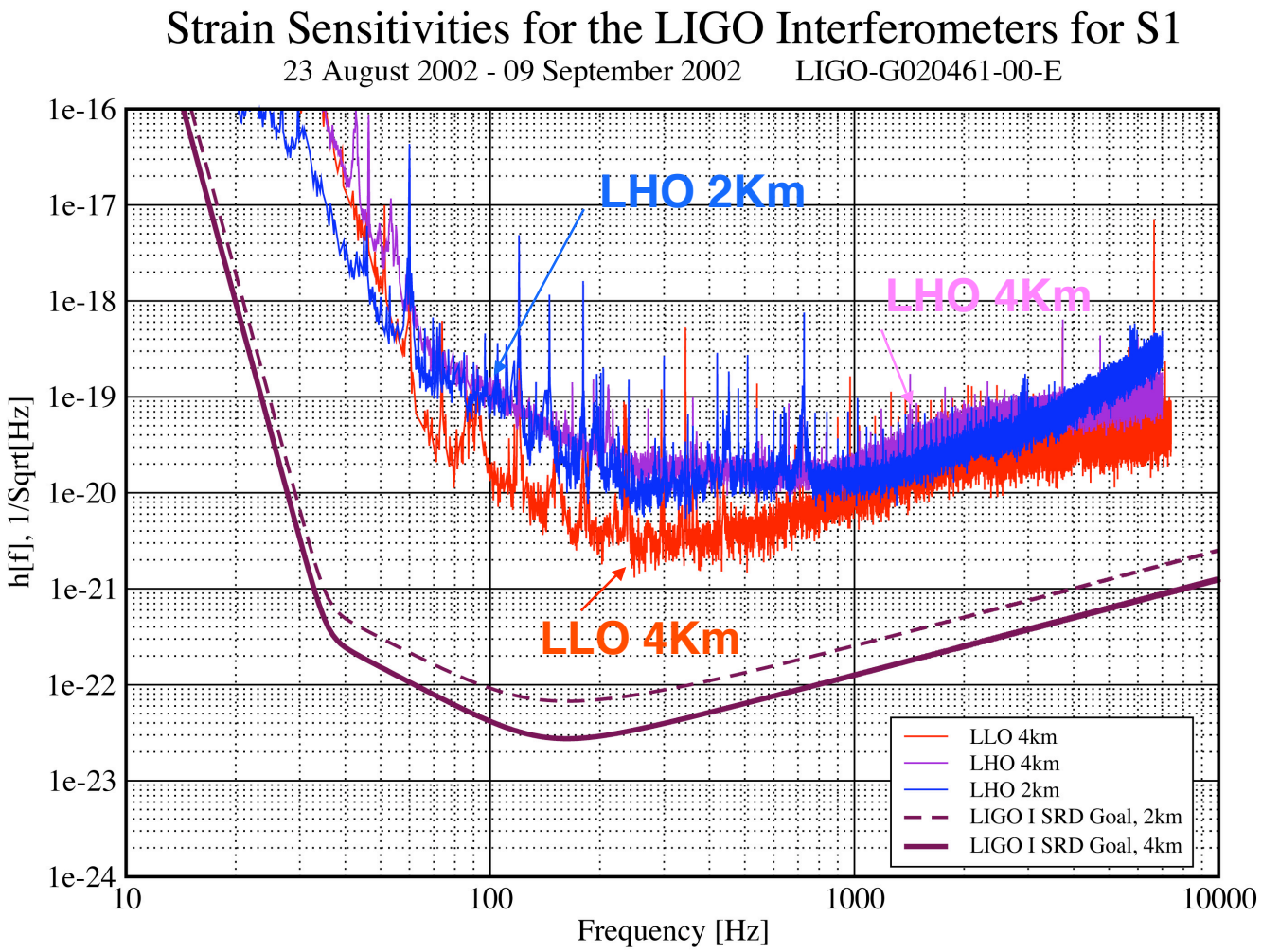

1. Compact binary sources

Coalescence inspirals

Detectability of coalescing binary sources during S1

(for optimal location & orientation relative to antenna pattern)

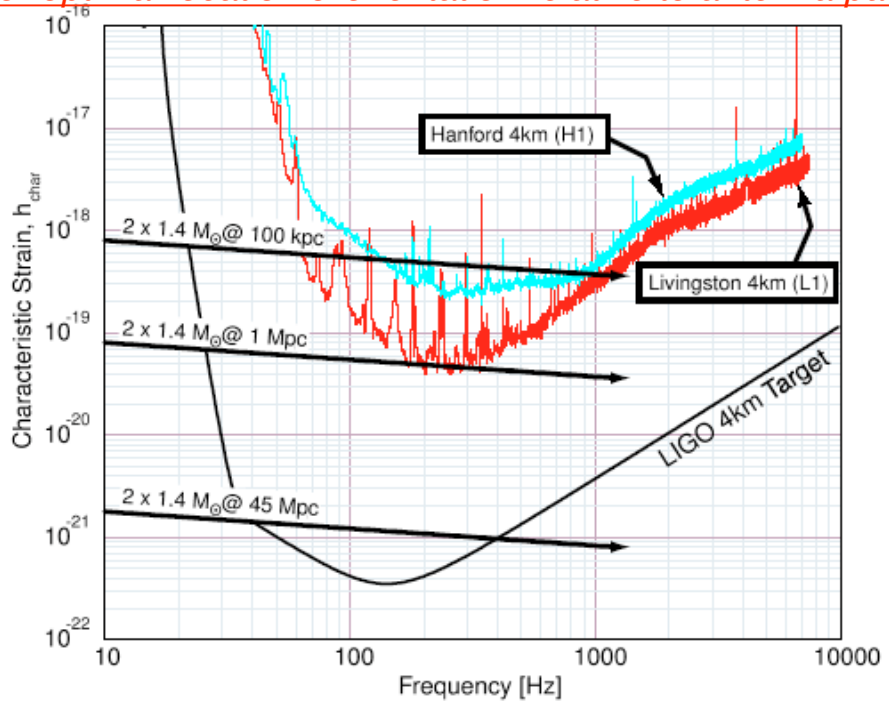

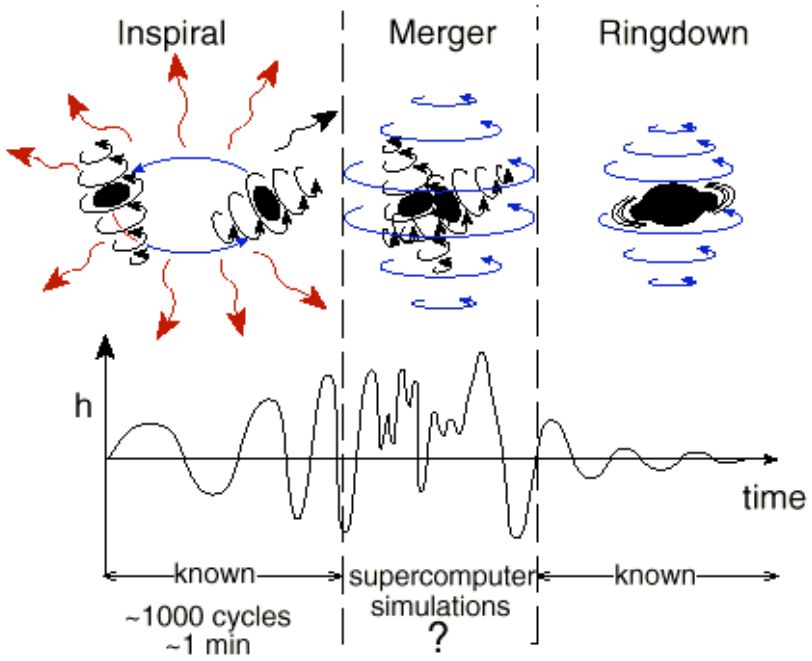

Compact binary sources
What is expected?

Brief Summary of Detection Capabilities of Mature LIGO Interferometers

• **Inspiral of NS/NS, NS/BH and BH/BH Binaries:** The table below [15] shows estimated rates $\mathcal{R}_{\rm gal}$ in our galaxy (with masses $\sim 1.4 M_\odot$ for NS and $\sim 10 M_\odot$ for BH), the distances $\mathcal{D}_{\rm I}$ and $\mathcal{D}_{\rm WB}$ to which initial IFOs and mature WB IFOs can detect them, and corresponding estimates of detection rates $\mathcal{R}_{\rm I}$ and $\mathcal{R}_{\rm WB}$; Secs. 1.1 and 1.2.

	NS/NS	NS/BH	BH/BH in field	BH/BH in globulars
$\mathcal{R}_{\rm gal}$, yr^{-1}	10^{-6}–10^{-4}	$\lesssim 10^{-7}$–10^{-4}	$\lesssim 10^{-7}$–10^{-5}	10^{-6}–10^{-5}
$D_{\rm I}$	20 Mpc	43 Mpc	100	100
$\mathcal{R}_{\rm I}$, yr^{-1}	$1 \times 10^{-4} - 0.03$	$\lesssim 1 \times 10^{-4} - 0.3$	$\lesssim 3 \times 10^{-3} - 0.5$	$0.03 - 0.5$
$D_{\rm WB}$	300 Mpc	650 Mpc	$z = 0.4$	$z = 0.4$
$\mathcal{R}_{\rm WB}$, yr^{-1}	$0.5 - 100$	$\lesssim 0.5 - 1000$	$\lesssim 10 - 2000$	$100 - 2000$

NOTE: Rate estimates *DO NOT* include most recent relativistic pulsar discovery, J0737-3039. · Estimates will increase by almost 10X (paper pending in *Nature*)

Table from: V. Kalogera (population synthesis articles) astro-ph/001238, astro-ph/ 0012172, astro-ph/ 0101047

Event search pipeline

Example from bursts -- prototypical for other searches

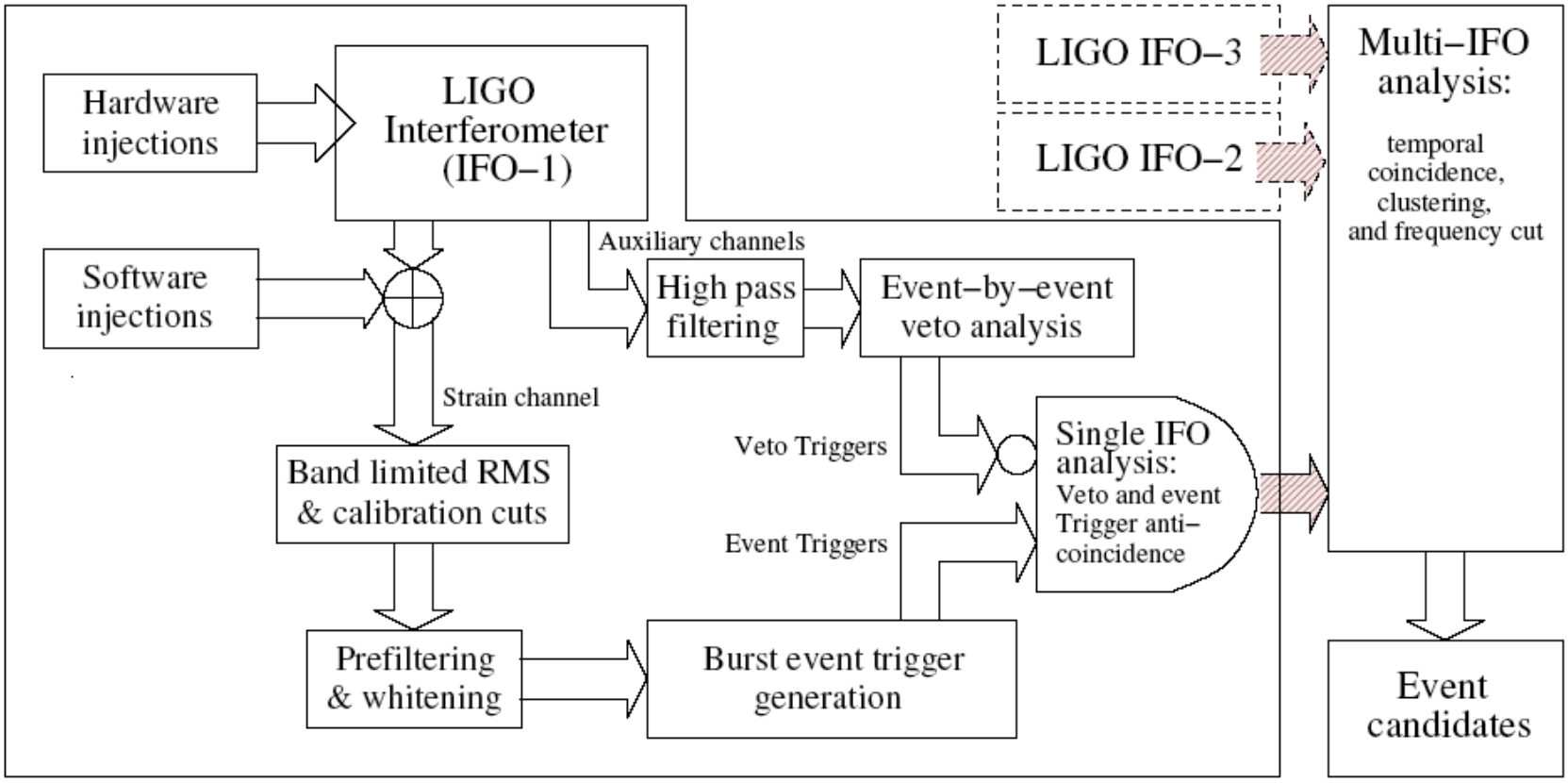

FIG. 2: Schematic outline of the S1 bursts analysis pipeline.

Search for compact binary sources

- Sources:
  - » Compact neutron star binaries undergoing orbital decay and coalescence.
  - » Masses, positions, orbital parameters, distances: ***unknown***
- Analysis goals:
  - » Develop and test an inspiral detection pipeline incorporating instrumental vetos and multi-instrument coincidence
  - » Obtain upper limit on the NS-NS inspiral rate
    - – For setting upper limits, need a source distribution model:
      - S1 range included Milky Way (our Galaxy) and LMC and SMC
      - *S2 range includes Andromeda*

Search for compact binary sources

- S1 Search method:
  - » Optimal Filtering used to generate GW candidates -- "triggers"
    - – Used only most sensitive two interferometers: H1 and L1. Distance to an optimally located & oriented SNR=8 source is L1: 176 kpc, H1: 46 kpc.
    - – Bank of 2110 second post-Newtonian stationary-phase templates for $1 < m_1 \leq m_2 < 3\ M_{sun}$ with 3% maximum mismatch for $(m_1 + m_{2)} < 4\ M_{sun}$
    - – Threshold on $\rho > 6.5$ and $\chi^2 < 5(8 + 0.03\ \rho^2)$ [8 frequency bins -- *see next slide*]
  - » Process ancillary channels to generate "vetoes" and cull data. Criteria established with playground dataset:
    - – Eliminate360s of contiguous science-mode intervals having large band-limited strain noise (3σ -- lowest band; 10σ -- higher bands) compared to run averages.
    - – H1: vetoed ±1 second windows from reflected port PD (avg arm length), eliminating 0.2% of data.
  - » ***Detection :*** require coincidence in time (<11 ms) and chirp mass (<1%) for triggers which are strong enough to be seen in both detectors
  - » ***Upper limit:*** set by measured detection efficiency at highest SNR event

Compact binary sources search

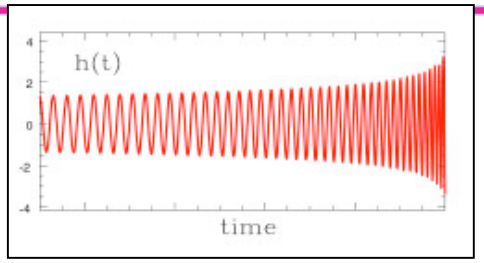

- Approach - Optimal Wiener filtering with chirp templates
  - Implemented for analysis of 1994 40m data, TAMA data

$$z(t) = x(t) + iy(t) = 4\int_0^\infty \frac{\tilde{h}_c^I(f)\tilde{s}^*(f)}{S_n(f)} e^{2\pi i f t} df \qquad \sigma^2 = 4\int_0^\infty \frac{|\tilde{h}_c^I(f)|^2}{S_n(f)} df$$

$$\rho(t) = \frac{|z(t)|}{\sigma}$$

  - Additionally require signal strength distributed in frequency-time plane according to a chirp
    - Select p = 8 frequency bands containing *equal signal strength*
    - Form χ^2 statistic to discriminate on integrated SNR -- z(t)/σ

$$\chi^2(t) = \frac{p}{\sigma^2}\sum^{p} |z_l(t) - z(t)/p|^2$$

Average SNR per band

    - Require: $\chi^2 < 5(p + 0.03\rho^2)$

      » essentially χ^2 per DOF of 5, but has weak SNR dependence due to template coverage

LIGO

- Compact Binaries - Diurnal variation of interferometer range during S1

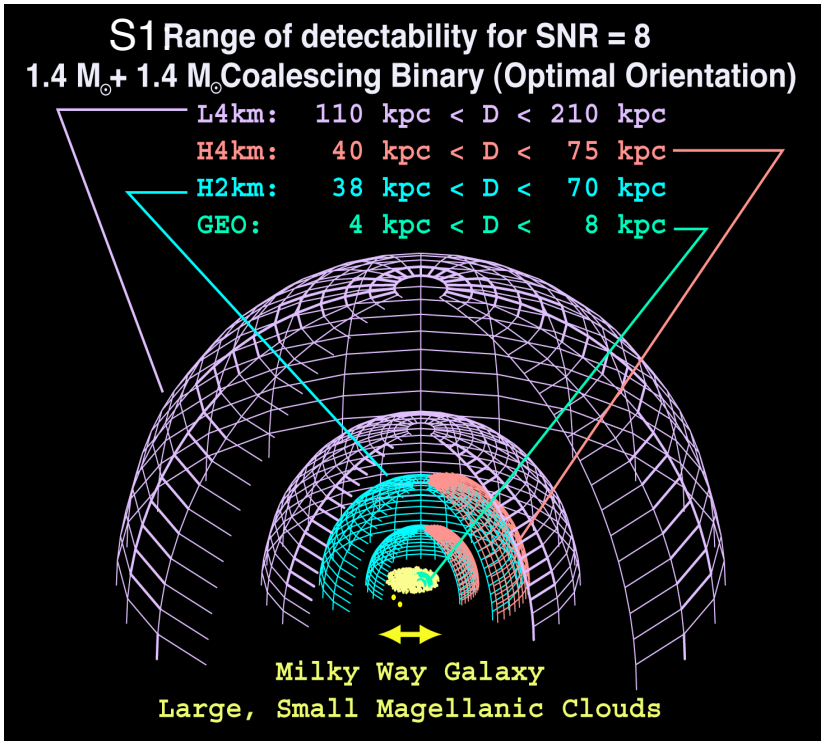

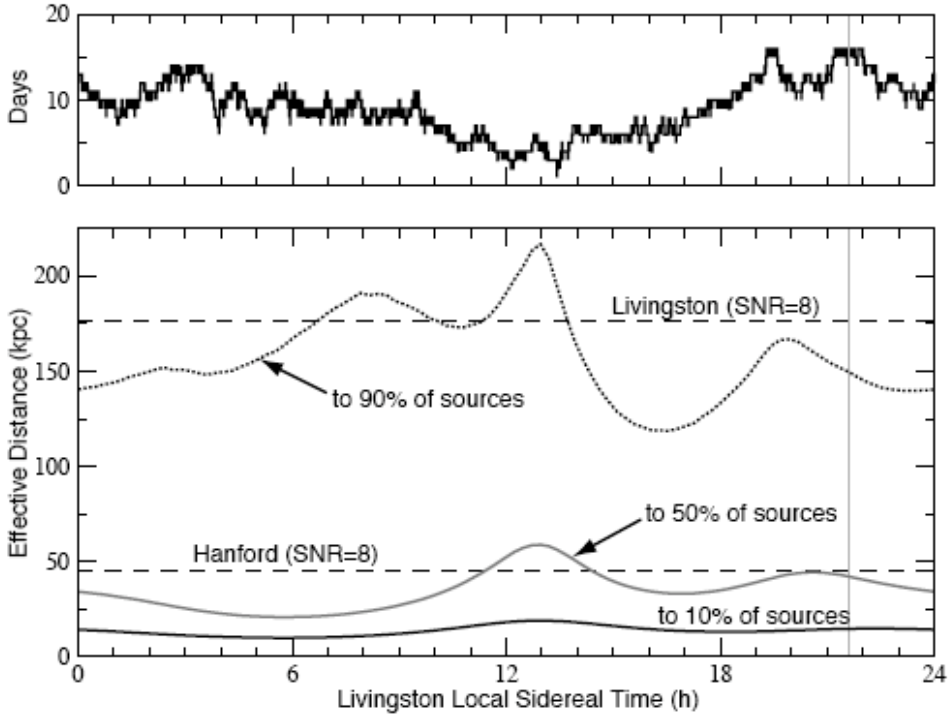

FIG. 2: Summary of detector status and sensitivity to the population of neutron stars described in Sec. as a function of sidereal time. For a given sidereal time, the upper panel shows the number of days during the run when at least one of the interferometers (H1 or L1) was collecting scientific data. For reference, the vertical dotted line indicates 05:00 UTC (corresponding to midnight at Livingston) on September 01, 2002. The lower panel shows the effective distance as measured in Livingston [and defined by Eq. ( )] to 10%, 50%, and 90% of the binary neutron star population described in Sec. . The horizontal dashed lines show the average distance at which an inspiral of $2 \times 1.4 M_{\odot}$ neutron stars, in the optimal direction and orientation with respect to each detector, would produce a signal-to-noise ratio of 8, *i.e.* 176 kpc for L1 and 46 kpc for H1.

Compact binary sources

Setting an upper limit on coalescence rate during S1

Catalog of largest SNR events after pipeline analysis

- Due to the sensitivity mismatch and low duty cycles during S1, highest SNR events were *only seen* in the Livingston interferometer

Date 2002	Time (UTC)	Detector(s)	SNR	χ^2/DOF	D_{eff} (kpc)	m_1 (M_{sun})	m_1 (M_{sun})
9/2	00:38:33.56	L1 only	15.9	4.3	95	1.31	1.07
9/8	12:31:38.28	L1 only (H1 on)	15.6	4.1	68	1.95	0.92
8/25	13:33:31.00	L1 only	15.3	4.9	101	3.28	1.16
8/25	13:29:24.25	L1 only	14.9	4.6	89	1.99	1.99
9/2	13:06:56.73	L1 only	13.7	2.2	96	1.38	1.38

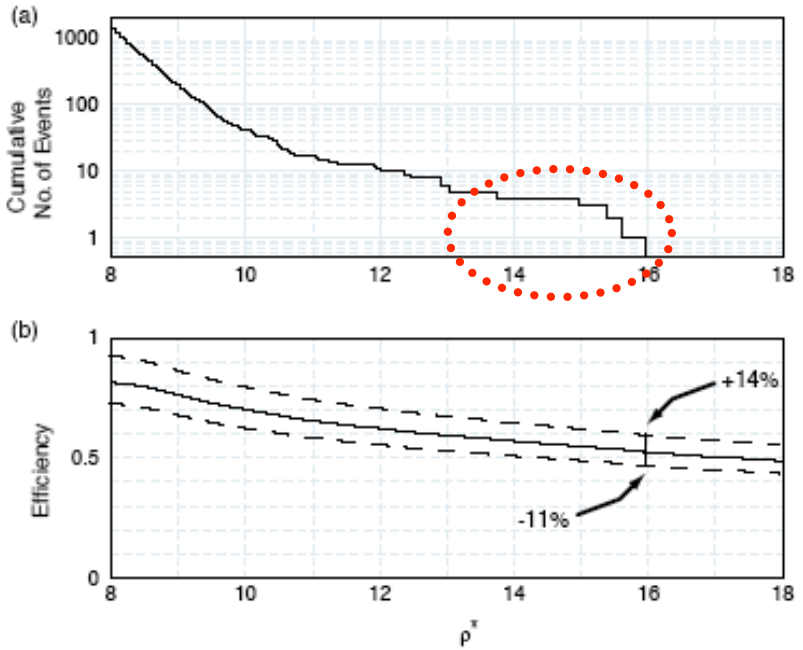

FIG. 6: Panel (a) shows the number of events in the data with SNR $> \rho^*$ as a function of ρ^*. The largest event has SNR = 15.9. Panel (b) shows the detection efficiency $\epsilon(\rho^*)$ for sources in the target population (Milky Way and Magellanic Clouds) as a function of ρ^*. The dashed lines indicate boundaries of our estimated systematic errors on the efficiency.

Compact binary sources

Discrimination against non-stationary noise artifacts

- Time dependence of signal strengths
  - »SNR - □
  - » □²
- Can distinguish true events vs. noise with same □ and □²

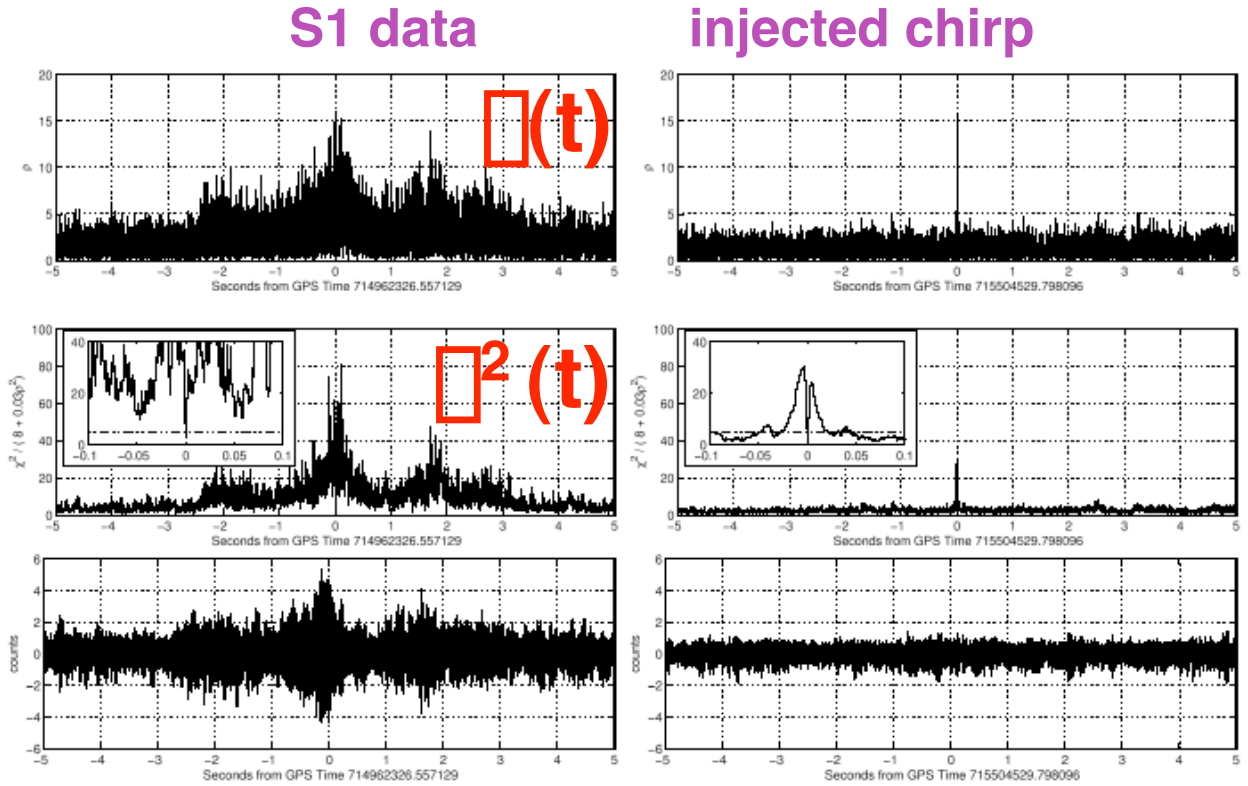

FIG. 5: Left Panels: The largest SNR candidate event seen during our search of the LIGO data. This candidate event occurred at a time when only L1 was in stable operation. The top panel shows the signal-to-noise time series, $\rho(t)$. Notice that $\rho(t) > 6.5$ many times in a ~ 5 second interval around the candidate event. The center panel shows $\chi^2/(p + 0.03\rho^2)$ as a function of time; notice $\chi^2/(p + 0.03\rho^2) > 5$ for ~ 5 seconds around the candidate event, but drops below this threshold right at the time of maximum ρ. The inset shows this more clearly for ± 0.1 second around the event where the threshold is indicated by a dot-dashed horizontal line. The bottom panel shows the time series for this candidate event after applying a high-pass filter with a knee frequency of 200 Hz. Notice the bursting behavior which does not look like an inspiral chirp signal. Right Panels: A simulated injection into the L1 data. This example was chosen for comparison with the largest SNR event shown in the left panels since it similar in mass parameters, detected signal to noise and χ^2. The instrument was behaving well at the time around the simulated injection. The top panel shows that $\rho(t) < 6.5$ except in close proximity to the signal detection time. The center panel shows $\chi^2/(p + 0.03\rho^2)$ as a function of time. Notice that it is much closer to threshold at all times around the simulated injection; this contrasts dramatically with the case of the candidate event shown in the left panels. The inset shows this more clearly for ± 0.1 seconds around the injection. The bottom panel shows the time series for this simulated injection after applying a high-pass filter with a knee frequency of 200 Hz. The inspiral chirp signal is not visible in the noisy detector output.

Compact binary sources
Upper limit on coalescence rate during S1

- Limit on binary neutron star coalescence rate:
  - »T = 236 h = 0.027 y
  - »N_G = 0.6 (= 1.13 L_G/L_G) $^{+\ 0.12}_{-\ 0.10}$ (systematic)
    = 0.5 (min)

$$\mathcal{R}_{90\%} = 2.303 \times \left(\frac{1\ \mathrm{y}}{T}\right)\left(\frac{1}{N_G}\right)\ \mathrm{y}^{-1}\ \mathrm{MWEG}^{-1}$$

$$\mathcal{R} < 1.7 \times 10^{2}\ \mathrm{y}^{-1}\ \mathrm{MWEG}^{-1}$$

No event candidates found in coincidence
90% confidence upper limit in the (m_1, m_2) range of 1 to 3 M_{sun}

- *26X lower than best published observational limit -- 40m prototype at Caltech[1]:*
  - »*$R_{90\%}$ (Milky Way) < 4400 /yr*
- *Comparable to recent TAMA analysis (1000 hr run)[2]:*
  - »*R < 123 /yr for MW Galaxy*

[1] *1994 data, Allen et al., Phys.Rev.Lett. 83 (1999) 1498*
[2] *TAMA Collaboration, 28th International Cosmic Ray Conference Proc, p3059.*

2. Periodic sources

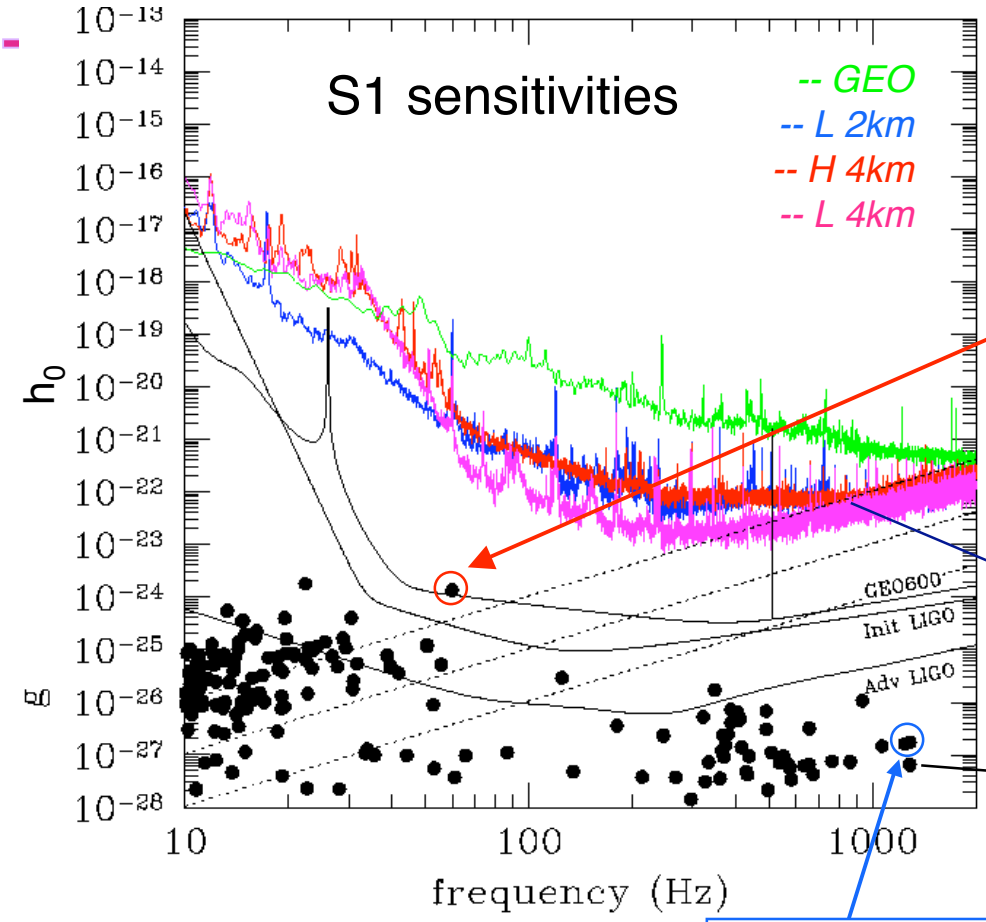

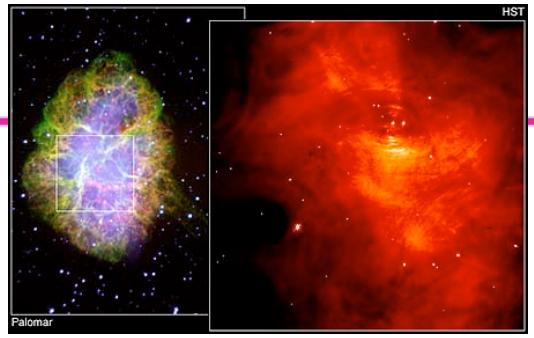

Crab pulsar

- h_0: Amplitude detectable with 99% confidence during observation time T

$$\langle h_0 \rangle = 11.4\sqrt{S_n(f_s)/T}$$

- *Limit of detectability for rotating NS with equatorial ellipticity, ε = ΔI/I$_{zz}$:*
  - *10^{-3} , 10^{-4} , 10^{-5} @ 10 kpc*
- ***Known** EM pulsars*
  - *Values of h_0 derived from measured spin-down*
    - *IF spin-down were entirely attributable to GW emissions*
    - *Rigorous astrophysical upper limit from energy conservation arguments*

PSR J1939+2134
P = 0.00155781 s
f_{GW} = 1283.86 Hz
$\dot{P}$ = 1.0519 10^{-19} s/s
D = 3.6 kpc

Search for Continuous Waves

- Source:
  PSR J1939+2134 (fastest known rotating neutron star) located 3.6 kpc from Earth
  - » Frequency of source: **known**
  - » Rate of change of frequency (spindown): **known**
  - » Sky coordinates (α, δ) of source: **known**
  - » Amplitude h_0: **unknown** (though spindown implies $h_0 < 10^{-27}$)
  - » Orientation ψ: **unknown**
  - » Phase, polarization ϕ, ι: **unknown**
- S1 Analysis goals:
  - » Search for emission at 1283.86 Hz (2 f_{EM}). Set upper limits on strain amplitude h_0.
  - » Develop and test an analysis pipeline optimized for efficient "known target parameter" searches (*time domain method*)
  - » Develop and test an efficient analysis pipeline that can be used for blind searches (*frequency domain method*)

Search for Continuous Waves

- S1 Search Methods:
  - »Performed for four interferometers: L1, H1, H2, GEO
  - »No joint interferometer result (timing problems, L1 best anyway)
  - »Time-domain method (sets Bayesian upper limit): <- ***REST OF THIS DISCUSSION***
    - – Heterodyne data (with fixed freq) to 4 samples/second
    - – Heterodyne data (with doppler/spindown) to 1 sample/minute
    - – Calculate $\chi^2(h_0, \square, \square, \square)$ for source model, antenna pattern
      Easily related to probability (noise Gaussian)
    - – Marginalize over $\square, \square, \square$ to get PDF for (and upper limit on) h_0
  - »Frequency-domain method (optimal for blind detection, frequentist UL):
    - – Take SFTs of (high-pass filtered) 1-minute stretches of GW channel
    - – Calibrate in the frequency domain, weight by average noise in narrow band
    - – Compute $\mathcal{F}$ == likelihood ratio (analytically maximized over $\square, \square, \square$)
    - – Obtain upper limit using Monte-Carlo simulations, by injecting large numbers of simulated signals at nearby frequencies

Power spectra near pulsar f_{GW}

Narrowband noise obeys Gaussian statistics

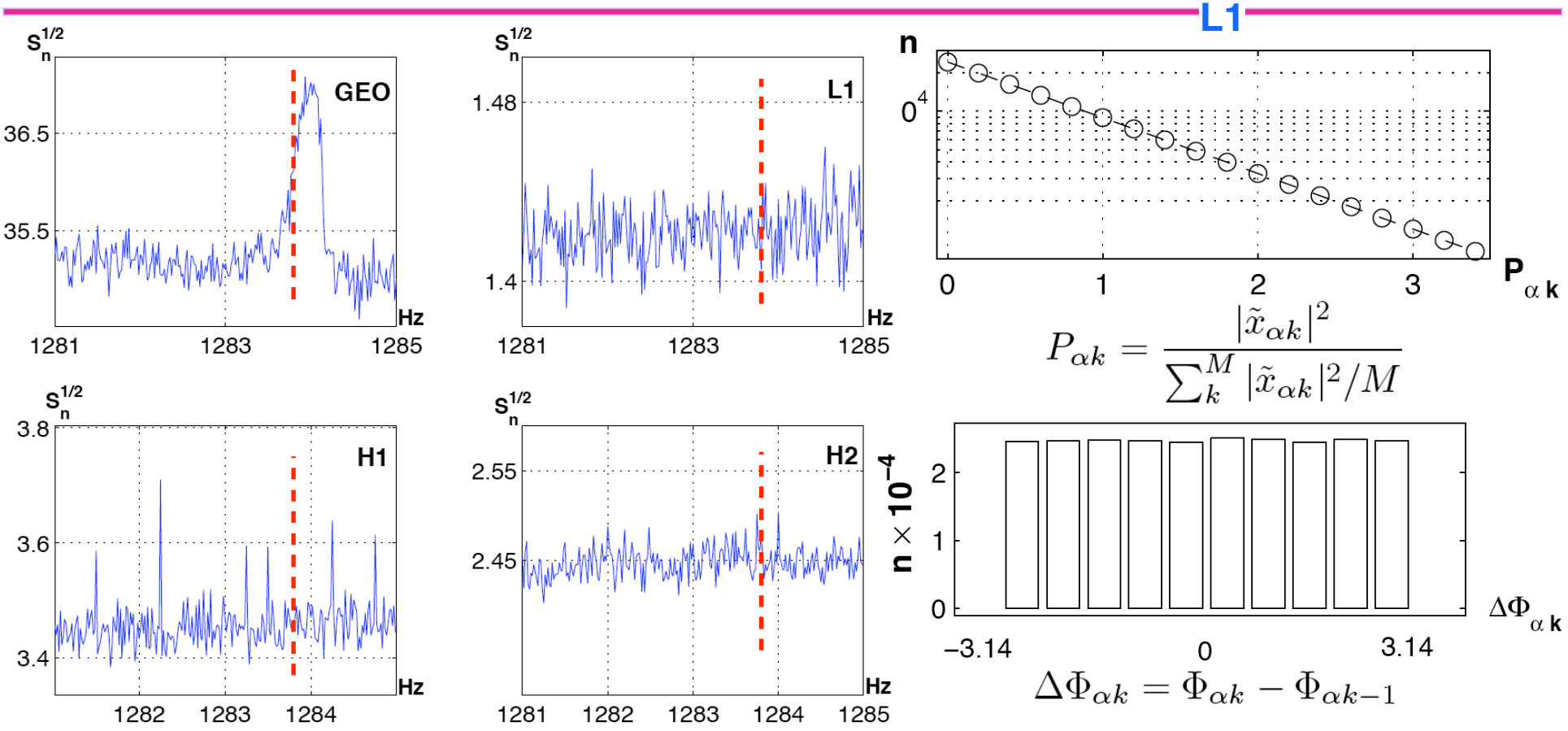

FIG. 5: $\sqrt{S_n}$ in a band of 4 Hz (starting at 1 281 Hz) using the entire S1 data set analyzed from the four interferometers. The noise $\sqrt{S_n}$ is shown in units of 10^{-20} $\mathrm{Hz}^{-1/2}$. The dashed vertical line indicates the expected frequency of the signal received from J1939+2134.

For Gaussian amplitude noise:
-exponential (Rayleigh) power dist.
-uniform phase dist.

Time domain behavior of data follow ideal behavior for Gaussian noise at pulsar f_{GW}

$$y(t_k;\mathbf{a}) = \frac{1}{4}F_+(t_k;\psi)h_0(1+\cos^2\iota)e^{i2\phi_0} - \frac{i}{2}F_\times(t_k;\psi)h_0\cos\iota\, e^{i2\phi_0}.$$

- *$y(t_k;\mathbf{a})$* is source model
  - ***a*** *= {h,□□,□₀}* - parameters

$$p(\mathbf{a}|\{B_k\}) \propto p(\mathbf{a})\exp\left[-\sum_k \frac{\Re\{B_k - y(t_k;\mathbf{a})\}^2}{2\sigma^2_{\Re\{B_k\}}}\right] \times \exp\left[-\sum_k \frac{\Im\{B_k - y(t_k;\mathbf{a})\}^2}{2\sigma^2_{\Im\{B_k\}}}\right]$$

- *B_k are the down-sampled & heterodyned data series*
- ✓ Residuals are normal deviates with N[0,1].
  - ✓ □² per DOF ~ 1

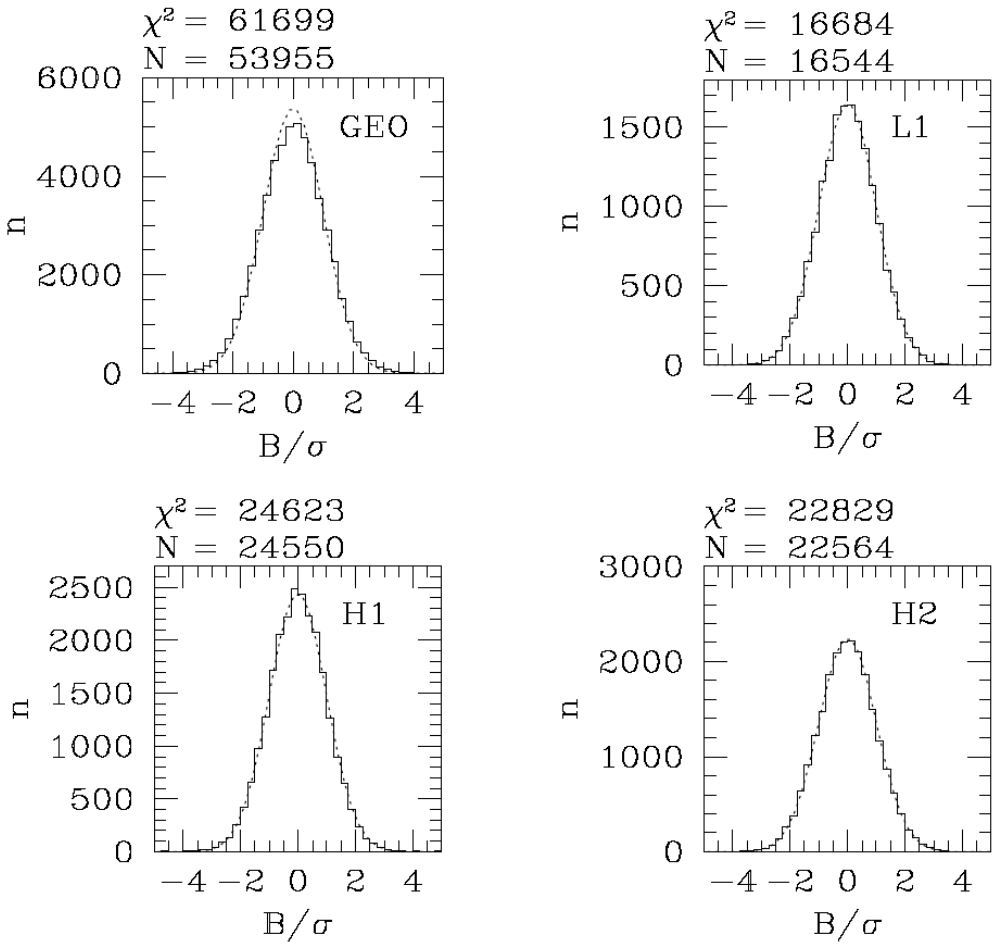

FIG. 7: Histograms of $B/\sigma = \Re(B_k)/\sigma_{\Re\{B_k\}} + \Im(B_k)/\sigma_{\Im\{B_k\}}$ for each interferometer. The dotted lines represent the expected Gaussian distribution, with $\mu = 0$ and $\sigma = 1$.

Bayesian upper limits from time domain analysis in concordance with frequentist results

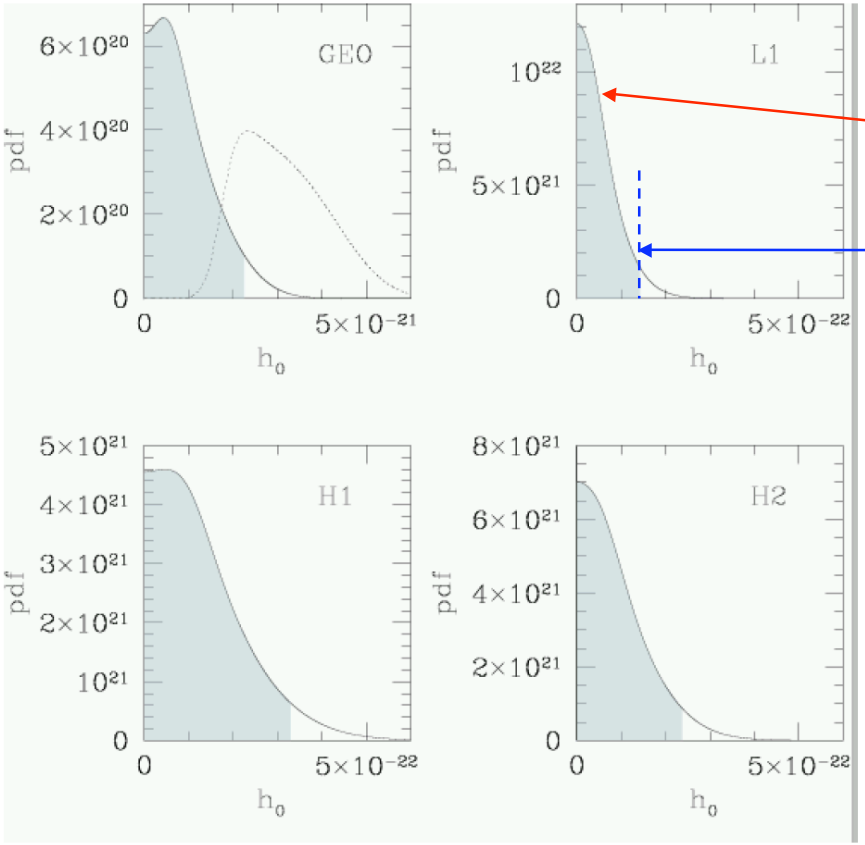

FIG. 8: For each interferometer, the solid line represents the marginalized posterior pdf for h_0 (PSR J1939+2134) resulting from the S1 data. The 95% upper limits (extent of the shaded region) are 2.2×10^{-21} for GEO, 1.4×10^{-22} for L1, 3.3×10^{-22} for H1 and 2.4×10^{-22} for H2. The dotted line in the GEO plot shows the posterior pdf of h_0 in the presence of a simulated signal injected into the GEO S1 data stream using $h_0 = 2.2 \times 10^{-21}$, $\phi_0 = 0°$, $\psi = 0°$ and $\iota = 0°$.

$$p(h_0|\{B_k\}) \propto \iiint p(\mathbf{a}|\{B_k\})\,\mathrm{d}\iota\,\mathrm{d}\psi\,\mathrm{d}\phi_0$$

$$0.95 = \int_0^{h_0^{95\%}} p(h_0|\{B_k\})\,\mathrm{d}h_0$$

IFO	Frequentist FDS	Bayesian TDS
GEO	$(1.9 \pm 0.1) \times 10^{-21}$	$(2.2 \pm 0.1) \times 10^{-21}$
L1	$(2.7 \pm 0.3) \times 10^{-22}$	$(1.4 \pm 0.1) \times 10^{-22}$
H1	$(5.4 \pm 0.6) \times 10^{-22}$	$(3.3 \pm 0.3) \times 10^{-22}$
H2	$(4.0 \pm 0.5) \times 10^{-22}$	$(2.4 \pm 0.2) \times 10^{-22}$

TABLE IV: Summary of the 95% upper limit values of h_0 for PSR J1939+2134. The frequency domain search (FDS) quotes a conservative frequentist upper limit and the time domain search (TDS) a Bayesian upper limit after marginalizing over the unknown ι, ψ and ϕ_0 parameters.

Upper limit on h_0 implies upper limit on ε

$$\epsilon^{95\%} = 2.9 \times 10^{-4} \left(\frac{10^{45}\ \mathrm{g\ cm^2}}{I_{zz}}\right)$$

4. Burst sources

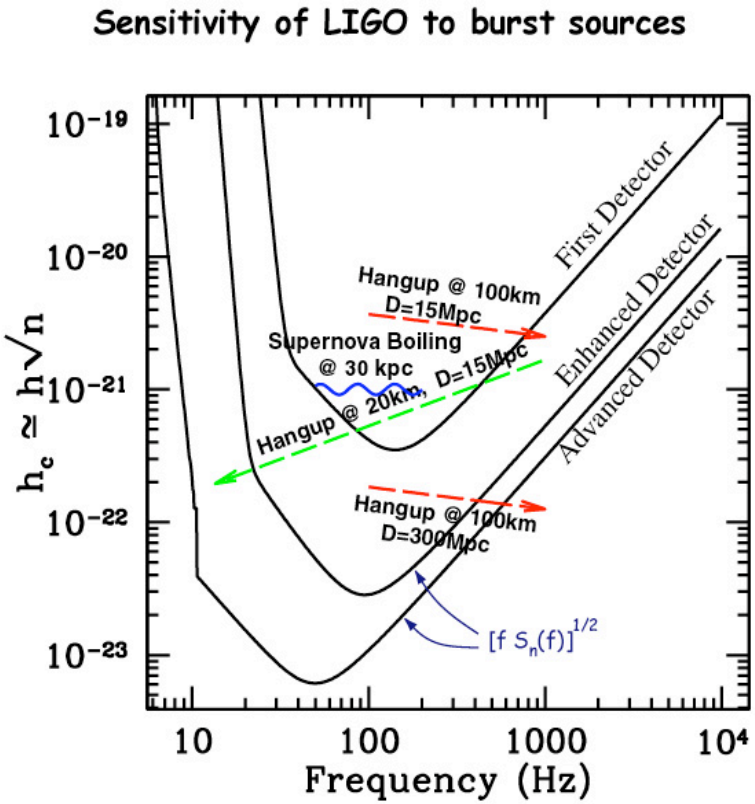

Expected SNe Rate

1/50 yr - our galaxy

3/yr - Virgo cluster

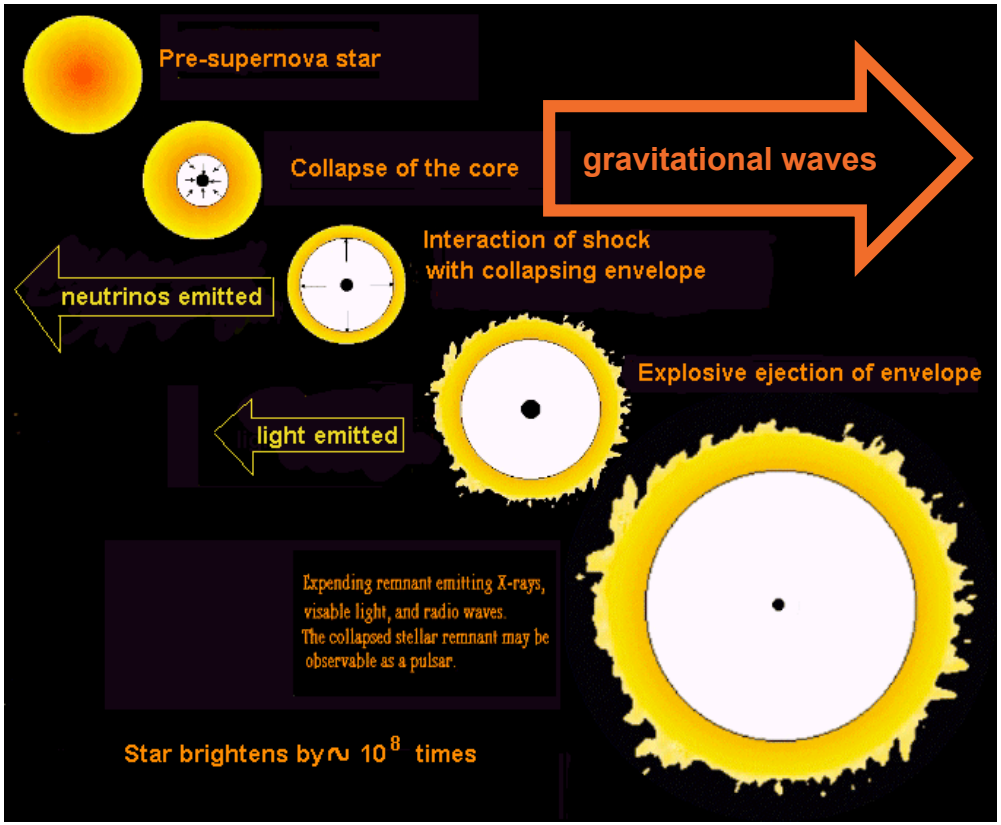

Burst Sources

- Sources:
  Phenomena emitting short transients of gravitational radiation of unknown waveform (supernovae, hypernovae, black hole mergers).
- Analysis goals:
  - » Do not bias search in favor of particular signal model(s)
  - » Search in a broad frequency band
  - » Establish bound on rate of instrumental events using [3X] coincidence techniques
  - » Interpret these bounds in terms of source/population models in rate versus strength plots

Burst Sources

- S1 Search methods:
  - » Create database of instrumental monitor triggers using DMT
  - » Create database of GW triggers using LDAS
    - – "TF-Clusters" algorithm identifies regions in the time-frequency plane with excess power (threshold on pixel power and cluster size) <- ***REST OF THIS DISCUSSION***
    - – "SLOPE" algorithm (time domain) is an optimal filter for a linear function of time with a 610 □sec rise-time.
  - » Veto GW trigger events by using instrumental monitors. (Thresholds set with playground data.)
  - » Use Monte-Carlo studies to determine detection efficiency as a function of signal strength and model
  - » Use time-shift analysis to estimate background rates, and Feldman-Cousins to set upper limits or confidence belts
  - » Upper bound: $R(h) \mu N / (\square(h)\, T)$ <- depends on h
    - N: number observed events
    - □(h): detection efficiency for amplitude h
    - T: observation time -- *livetime*
    - Proportionality constant depends on confidence level (CL) -- of order 1 for 90%

Efficiency determination using Monte Carlo

TFCLUSTERS -- Single and triple coincidences

Optimal Wave & Polarization Orientation

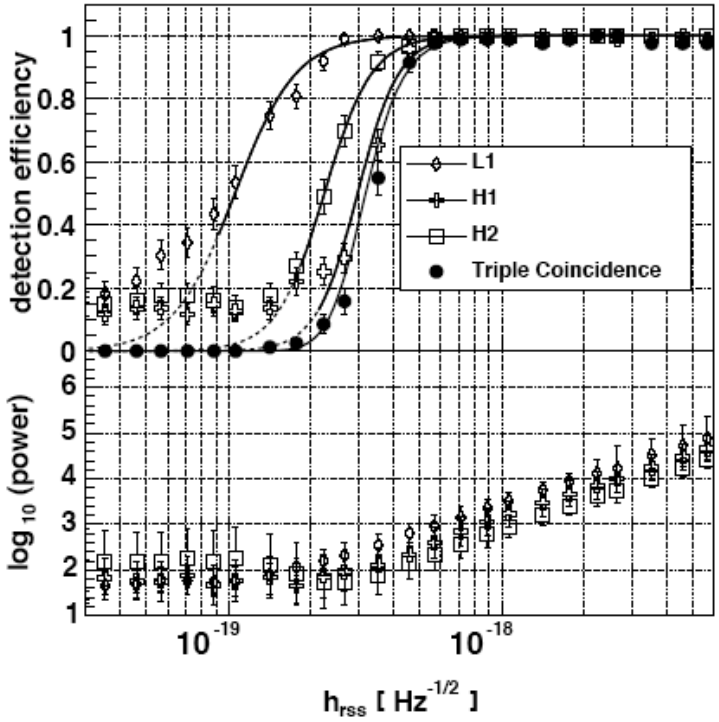

FIG. 10: The response of the TFCLUSTERS event trigger generator to Gaussian bursts with $\tau = 1$ ms, embedded in S1 data, as a function of the root-sum-square strain h_{rss}. Upper plot: Average burst detection efficiency. The efficiencies were evaluated through simulations of burst waveforms with optimal wave direction and polarization, injected into S1 data. The simulated data points are fitted to sigmoid curves, shown, in the region where the efficiency is not dominated by random noise triggers. The curve for the triple-coincidence is the product of the single-detector efficiency curves, and can be directly compared with the triple-coincidence simulation data points. Lower plot: Average detected signal strength for each of the three LIGO detectors.

Detection threshold vs. frequency

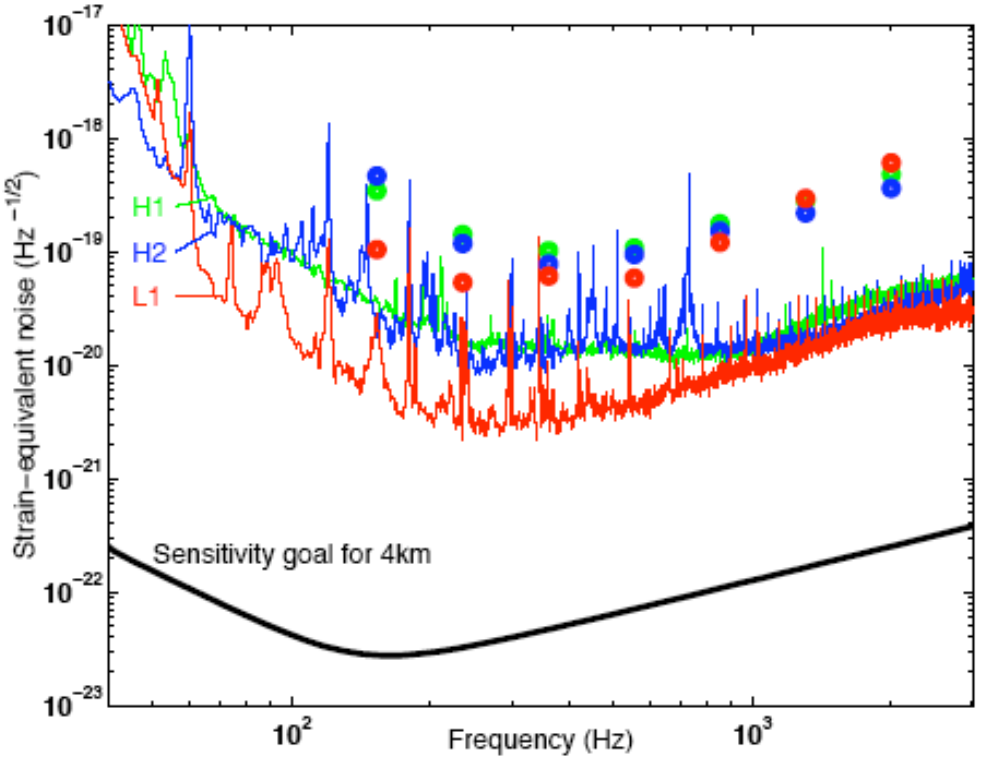

FIG. 1: Typical sensitivities of the three LIGO detectors during the S1 data run, in terms of equivalent strain noise amplitude density. The points are the root-sum-square strain (h_{rss}) of sine-Gaussian bursts for which our TFCLUSTERS analysis pipeline is 50% efficient, as reported in section V B.

$$h_{rss} \equiv \sqrt{\int |h|^2 dt}$$
$$\sqrt{\sqrt{\pi/2}\tau}h_0 \text{ (Gaussians)}$$
$$= \sqrt{Q/(4\sqrt{\pi}f_0)}h_0 \text{ (sine-Gaussians)}$$

Background Estimation and Upper Limits Analysis
TFCLUSTERS algorithm -- Time shift analysis

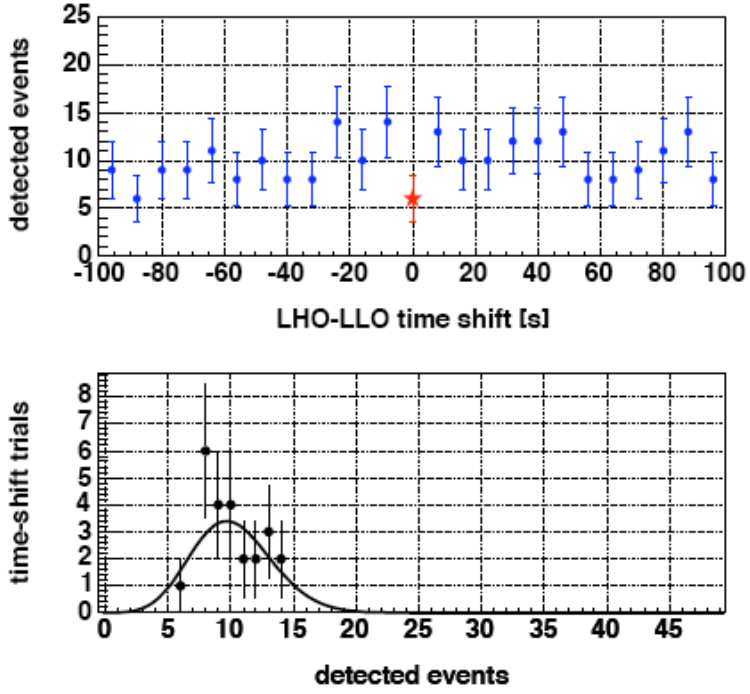

FIG. 6: Time-shifted triple coincident events from TFCLUSTERS event triggers, as a function of an artificial time shift introduced between the Hanford (LHO) and Livingston (LLO) sites. Top: Number of events versus time shift, in 8 second steps; the point at zero time shift is the number of true triple coincident events. Bottom: Histogram of the number of time-shifted coincident events, with the Poisson fit overlaid (the zero time shift point is excluded). In both plots, the error bars are Poissonian.

TABLE I: Confidence bands on the number of excess events in the S1 run (35.5 hours of observation time) from the TFCLUSTERS pipeline.

Coincident events	6
Background	10.1 ± 0.6
90% confidence band	$0 - 2.3$
95% confidence band	$0 - 3.5$
99% confidence band	$0 - 5.9$

Efficiency vs. Rate

Interpret result as an upper limit on event rate vs. rss strain

Efficiency depends on signal frequency content

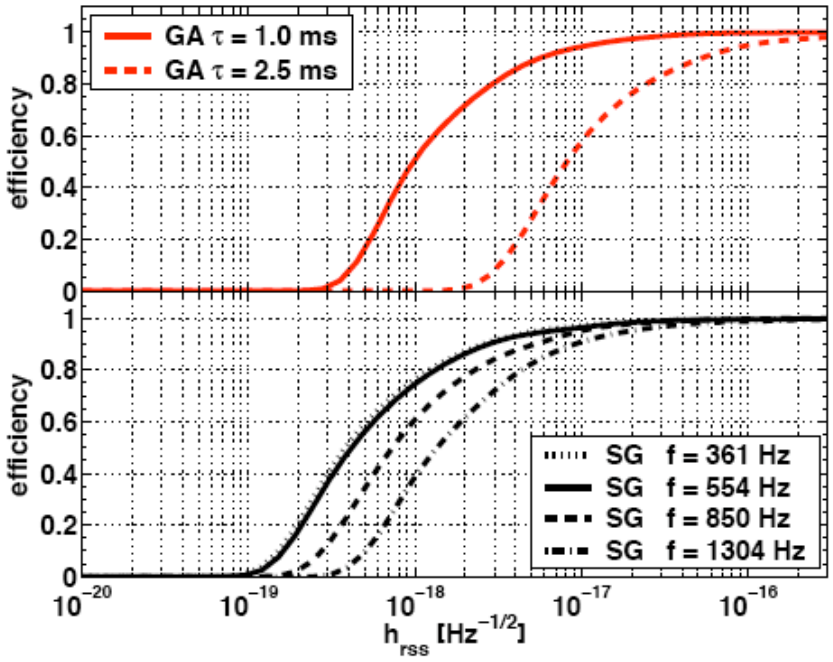

FIG. 13: Burst detection efficiency for triple coincidence as a function of h_{rss}, using the TFCLUSTERS event trigger generator, averaging over wave directions and polarizations, for six different waveforms: GA refers to the Gaussians defined in Eqn. 5.1 and SG to the sine-Gaussians defined in Eqn. 5.2.

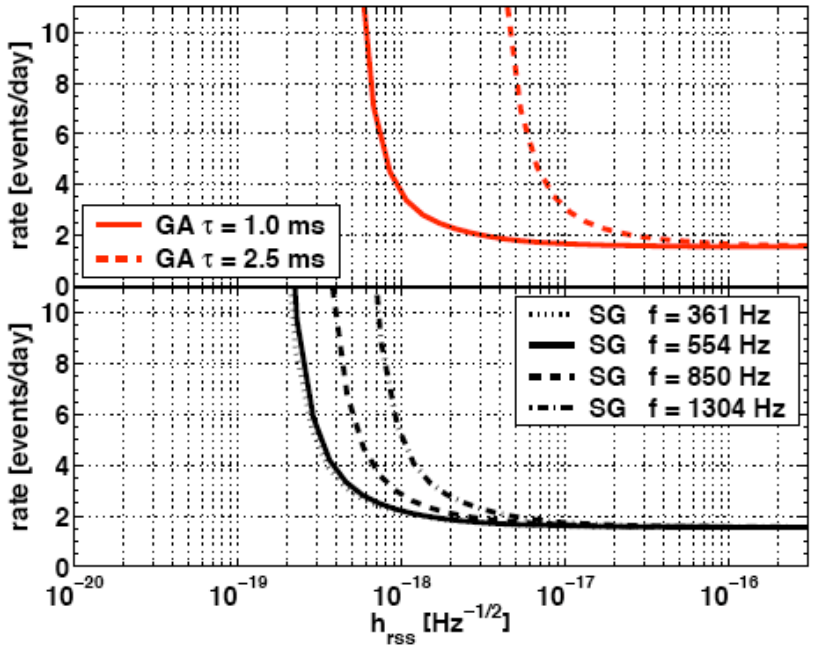

FIG. 15: Rate versus h_{rss} for detection of specific waveforms using the TFCLUSTERS event trigger generator. The region above and to the right of the curves is excluded at 90% confidence level or greater. The effect of the 20% uncertainty in the detector response is included. Top: For Gaussians with $\tau = 1.0$ ms and $\tau = 2.5$ ms. Bottom: For sine-Gaussians with $Q = 9$ and central frequency $f_0 = 361$, 554, 850 and 1304 Hz.

4. Stochastic gravitational wave background

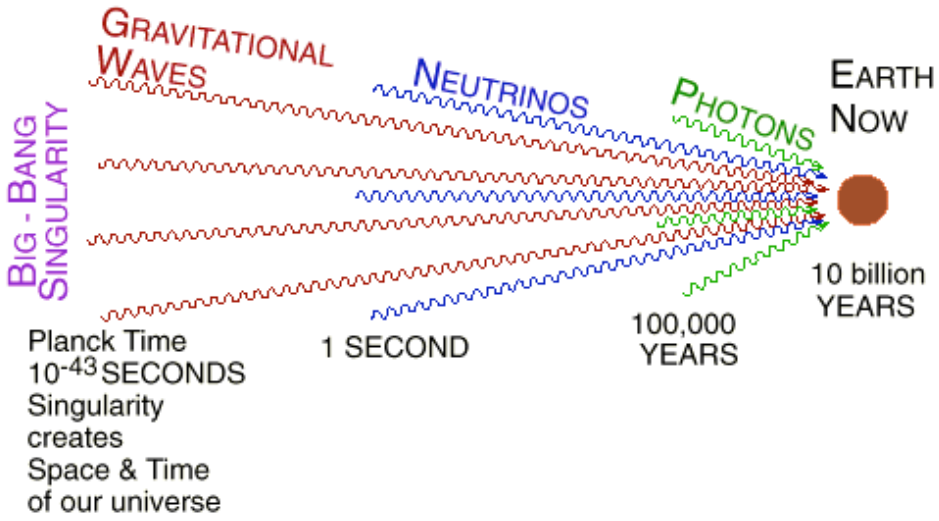

- Detect by cross-correlating interferometer outputs in pairs
  - Hanford - Livingston, Hanford - Hanford
- Good sensitivity requires:
  - $\Omega_{GW} \geq 2D$ (detector baseline)
  - $f \leq 40$ Hz for L - H pair
- Initial LIGO limiting sensitivity: $\Omega < 10^{-6}$

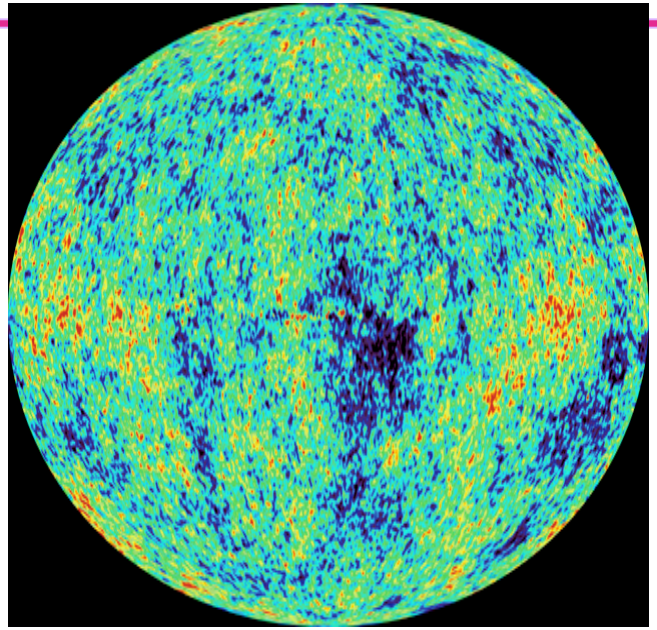

Analog from cosmic microwave background -- WMAP 2003

$$\int_0 d(\ln f)\ \Omega_{GW}(f) = \frac{\rho_{GW}}{\rho_{critical}}$$

The integral of $[1/f \cdot \Omega_{GW}(f)]$ over all frequencies corresponds to the fractional energy density in gravitational waves in the Universe

Stochastic background radiation

- Sources
  - » Early universe sources (inflation, cosmic strings, etc) produce very weak, non-thermal unpolarized, isotropic, incoherent background spectrum
  - » Contemporary sources (unresolved SN & inspiral sources) produce power-law spectrum
  - » Indirect constraints on fractional energy density $\Omega_{GW}(f) < 10^{-5}$
- Analysis goals:
  - » Directly constrain $\Omega_{GW}(f)$ for 40 Hz ≤ f ≤ 300 Hz
  - » Investigate instrumental correlations

Stochastic background radiation

- S1 search method
  - » Look for correlations between pairs of detectors
  - » Analyze data in (2-detector coincident) 900-second stretches
  - » Partition each of these into 90-second stretches to characterize statistics
  - » Window, zero pad, FFT, estimate power spectrum for 900 sec
  - » Notch out frequencies containing instrumental artifacts
    - – Very narrow features - 0.25 Hz bins
    - – $n \times 16$ Hz, $n \times 60$ Hz, 168.25 Hz, 168.5 Hz, 250 Hz
  - » Find cross-correlation with filter optimal for $\Omega_{GW}(f) \mu f^0$ (constant)
  - » Extensive statistical analysis to set 90% confidence upper limit

Stochastic background radiation

- Current best upper limits:
  - » Inferred: From Big Bang nucleosynthesis: (Kolb et al., 1990) $\int \Omega_{GW}(f)\ d\ln f < 1.10^{-5}$
  - » *Measured:* Garching-Glasgow interferometers (Compton et al. 1994): $\Omega_{GW}(f) < 3.10^{5}$
  - » *Measured*: EXPLORER-NAUTILUS (cryogenic bars -- Astone et al., 1999): $\Omega_{GW}(907Hz) < 60$

Cross-correlation technique enables one to "dig" signal below individual interferometer noise floors

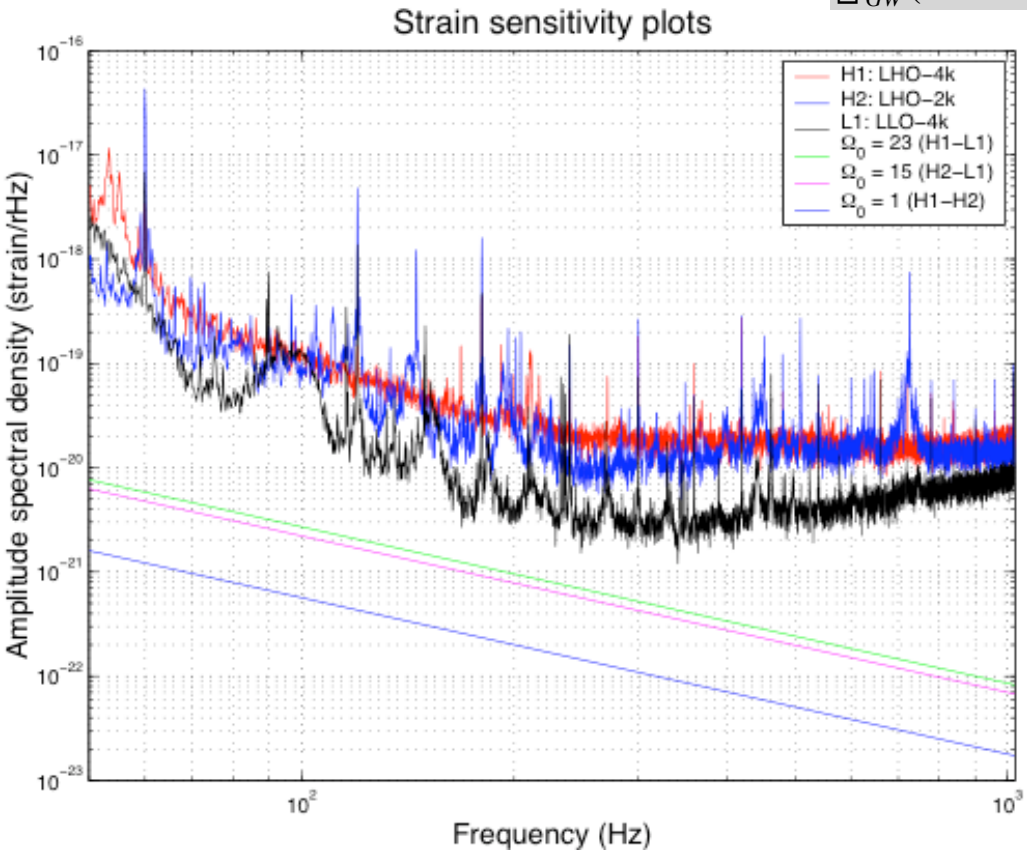

Stochastic background radiation

Measurement technique: detector cross-correlation

$$Y \equiv \int_{-T/2}^{T/2} dt_1 \int_{-T/2}^{T/2} dt_2\, s_1(t_1)\, Q(t_1 - t_2)\, s_2(t_2)$$

$$\mu_Y \equiv \langle Y \rangle = \frac{T}{2} \int_{-\infty}^{\infty} df\, \gamma(|f|) S_{\rm gw}(|f|)\, \widetilde{Q}(f)$$

$$\sigma_Y^2 \equiv \langle (Y - \langle Y \rangle)^2 \rangle \approx \frac{T}{4} \int_{-\infty}^{\infty} df\, P_1(|f|)\, |\widetilde{Q}(f)|^2\, P_2(|f|)$$

$$\widetilde{Q}(f) = \mathcal{N} \frac{\gamma(|f|)}{|f|^3 P_1(|f|) P_2(|f|)}$$

$$S_{\rm gw}^{1/2}(f) = 5.6 \times 10^{-22}\, h_{100} \sqrt{\Omega_0} \left(\frac{100\,{\rm Hz}}{f}\right)^{3/2} {\rm Hz}^{-1/2}$$

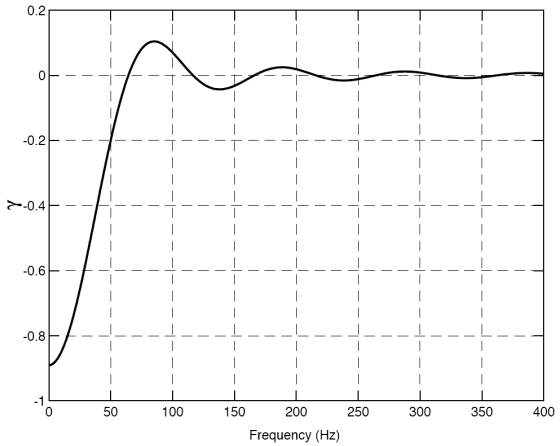

FIG. 2: Overlap reduction function between the LIGO Livingston and the LIGO Hanford sites. The value of $|\gamma|$ is a little less than unity at 0 Hz because the interferometer arms are not exactly co-planar and co-aligned between the two sites.

- Mean of Y proportional to Ω_{GW}
- Variance due to instrument noise floors
- Optimal filter, Q(f), depends on noise floors and a geometrical factor relating detector orientations and antenna patterns
  - » Perfectly aligned co-located detectors have $\gamma(f) == 1$

Stochastic background radiation
Selection of measurement band

- Contribution to total SNR, □/□$_Y$, as a function of frequency for the three detector pairs

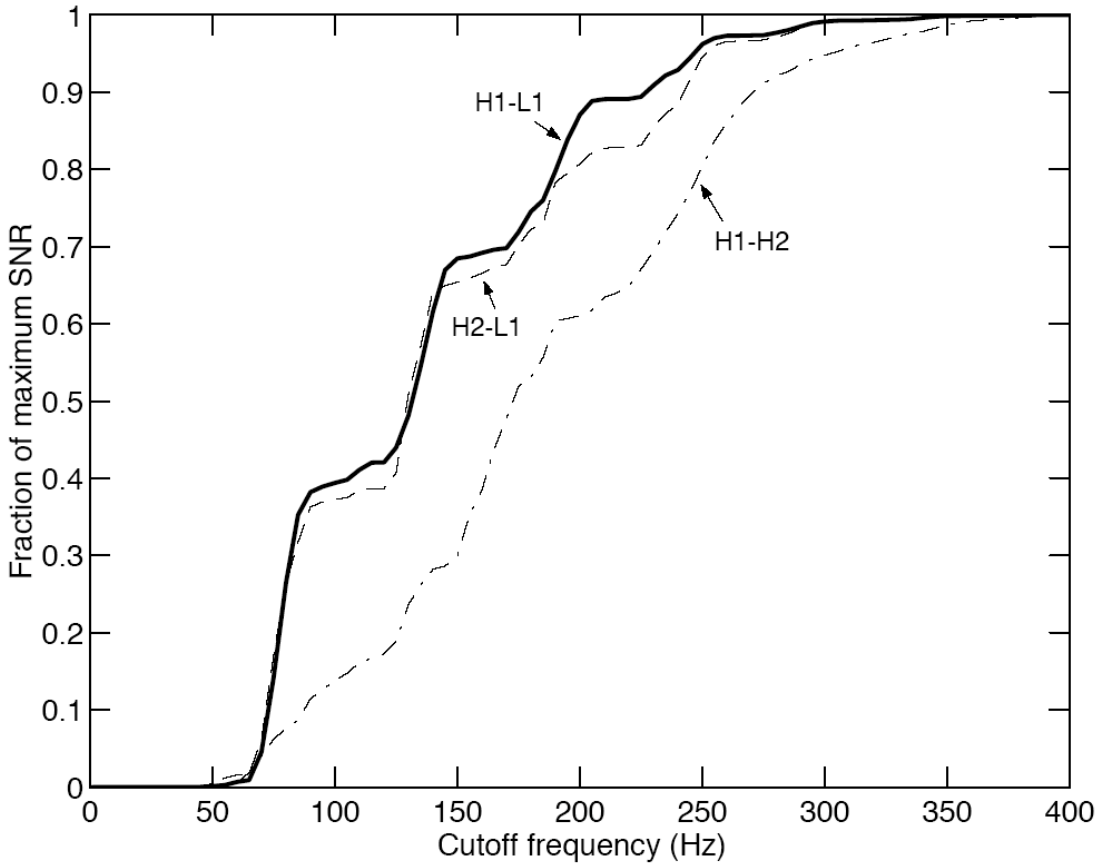

FIG. 6: Curves show the fraction of maximum expected signal-to-noise ratio as a function of cut-off frequency, for the three interferometer pairs. The curves were made by numerically integrating Eq. 4.11 from a few Hz up to the variable cut-off frequency, using the strain sensitivity spectra shown in Fig. 1.

Stochastic background radiation

Best upper limit on Ω_{GW} provided by H2-L1

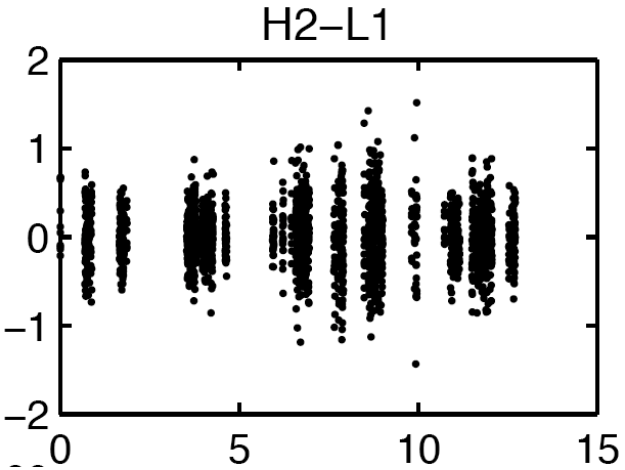

Days of observation
S1Measurements over S1

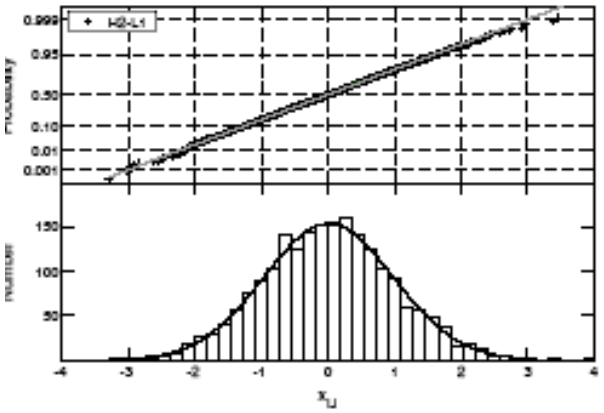

Normalized residuals over S1 run

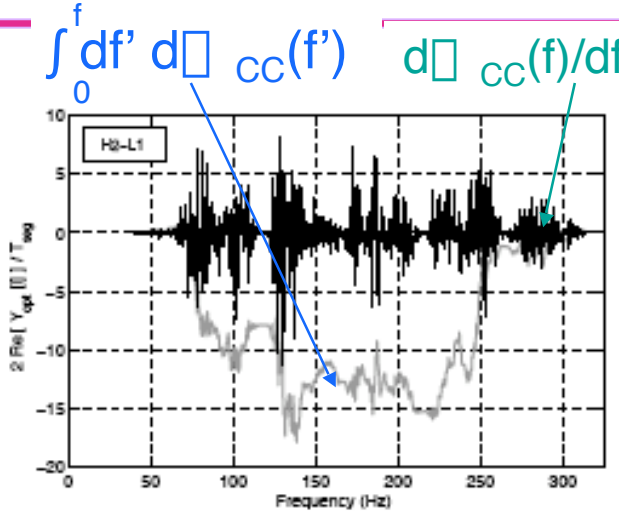

Run-averaged spectrum of cross correlation (CC)

Interferometer pair	$\widehat{\Omega}_{\rm eff}\, h_{100}^2$	$\widehat{\Omega}_{\rm eff}\, h_{100}^2/\widehat{\sigma}_{\Omega,\rm tot}$	90% confidence interval on $\Omega_{\rm eff}\, h_{100}^2$	90% confidence upper limit	$\chi^2_{\rm min}$ (per dof)	Frequency range	Observation time
H1-H2	-8.3	-8.8	$[-9.9 \pm 2.0\,,\ -6.8 \pm 1.4]$	–	4.9	$40 - 300$ Hz	100.25 hr
H1-L1	32	1.8	$[2.1 \pm .42\,,\ 61 \pm 12]$	$\Omega_0\, h_{100}^2 \leq 55 \pm 11$	0.96	$40 - 314$ Hz	64 hr
H2-L1	0.16	0.0094	$[-30 \pm 6.0\,,\ 30 \pm 6.0]$	$\Omega_0\, h_{100}^2 \leq 23 \pm 4.6$	1.0	$40 - 314$ Hz	51.25 hr

TABLE II: Measured 90% confidence intervals and upper limits for the three LIGO interferometer pairs, assuming $\Omega_{\rm gw}(f) \equiv \Omega_0 = \text{const}$ in the specified frequency band. For all three pairs we compute a confidence interval according to Eq. 5.25. For the LHO-LLO pairs, we are confident in assuming the instrumental correlations are insignificant, and an upper limit on a stochastic gravitational background is computed according to Eq. 5.26. Our established upper limit comes from the H2-L1 pair. The $\pm$ error bars given for the confidence intervals and upper limit values derive from a $\pm 10\%$ uncertainty in the calibration magnitude of each detector; see Sec. VI and Table IV. The $\chi^2_{\rm min}$ per degree of freedom values are the result of a frequency-domain comparison between the measured and theoretically expected cross-correlations, described in Sec. V E.

Summary of S1
The methodology of LIGO science

- The first upper limits results have been obtained using the LIGO interferometers in coincidence. These have resulted in four ***methodology*** papers:

  Papers submitted to *Physical Review D*:

  ‡ *"Analysis of LIGO data for gravitational waves from binary neutron stars", gr-qc/0308069*

  ‡ *"Setting upper limits on the strength of periodic gravitational waves using the first science data from the GEO600 and LIGO detectors", gr-qc/0308050*

  Papers under internal collaboration review:

  ‡ *"First upper limits on gravitational wave bursts from LIGO"*

  ‡ *"Analysis of First LIGO Science Data for Stochastic Gravitational Waves"*

- A paper describing the instruments has also been written.

  ‡ *"Detector Description and Performance for the First Coincidence Observations between LIGO and GEO", gr-qc/0308043*, ***accepted for publication by Nuclear Instruments and Methods***

Plans for S2 and beyond

- Inspiral
  - » (If no detections) get better upper limit, making use of longer observation time, additional sources in Andromeda
  - » Improved data quality cuts and statistical testing; coherent analysis
  - » Search for non-spinning BHs up to ~20 solar masses (or UL)
  - » Search for MACHO binaries (low mass BHs) in Galactic Halo
- Bursts
  - » "Eyes wide open" search for signals in the 1-100 msec duration
  - » Triggered search for correlations with GRBs
  - » Modeled search for
    - – Black hole ringdown
    - – Supernovae waveform catalog
  - » Four-way coincidence with TAMA
  - » Introduce amplitude constraints, tighter time coincidence windows, cross-correlation of time-series data from multiple interferometers near event candidates for better discrimination
- Periodic sources

  Time domain method:
  - » Upper limits on all known pulsars > 50 Hz
  - » Search for Crab
  - » Develop specialized statistical methods (Metropolis-Hastings Markov Chain) to characterize PDF in parameter space

  Frequency domain method
  - » Search parameter space (nearby all-sky broadband + deeper small-area)
  - » Specialized search for SCO-X1 (pulsar in binary)
  - » Incoherent searches: Hough, unbiased, stack-slide
- Stochastic
  - » May optimally filter for power-law spectra: $\Omega_{GW}(f) \propto f^{\alpha}$
  - » Correlate ALLEGRO-LLO
  - » Technical improvements: apply calibration data once/minute, overlapping lower-leakage windows, study H1-H2 correlations in more detail.

Sensitivity Improvements

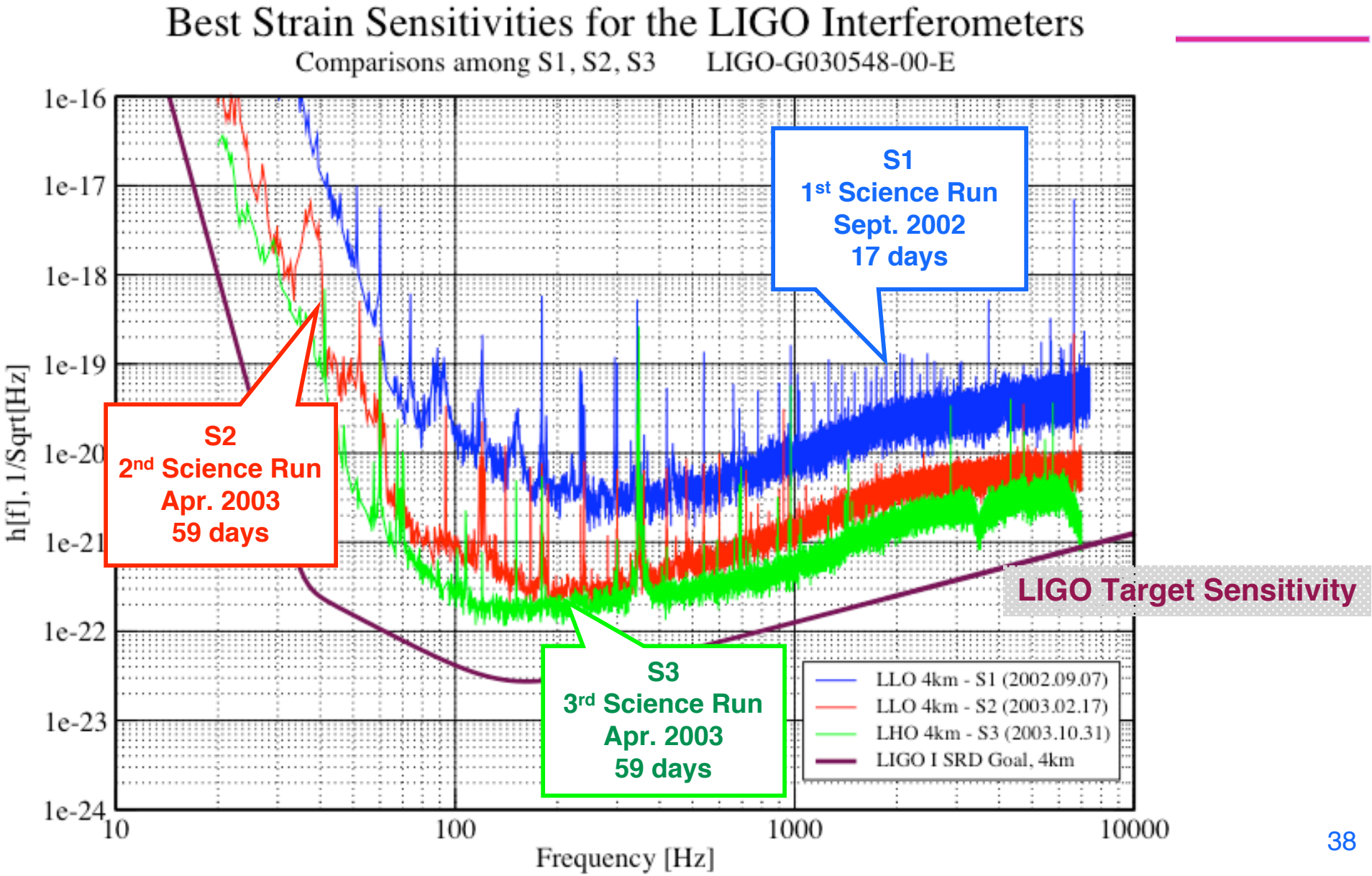

S2 -- L1 reaches Andromeda

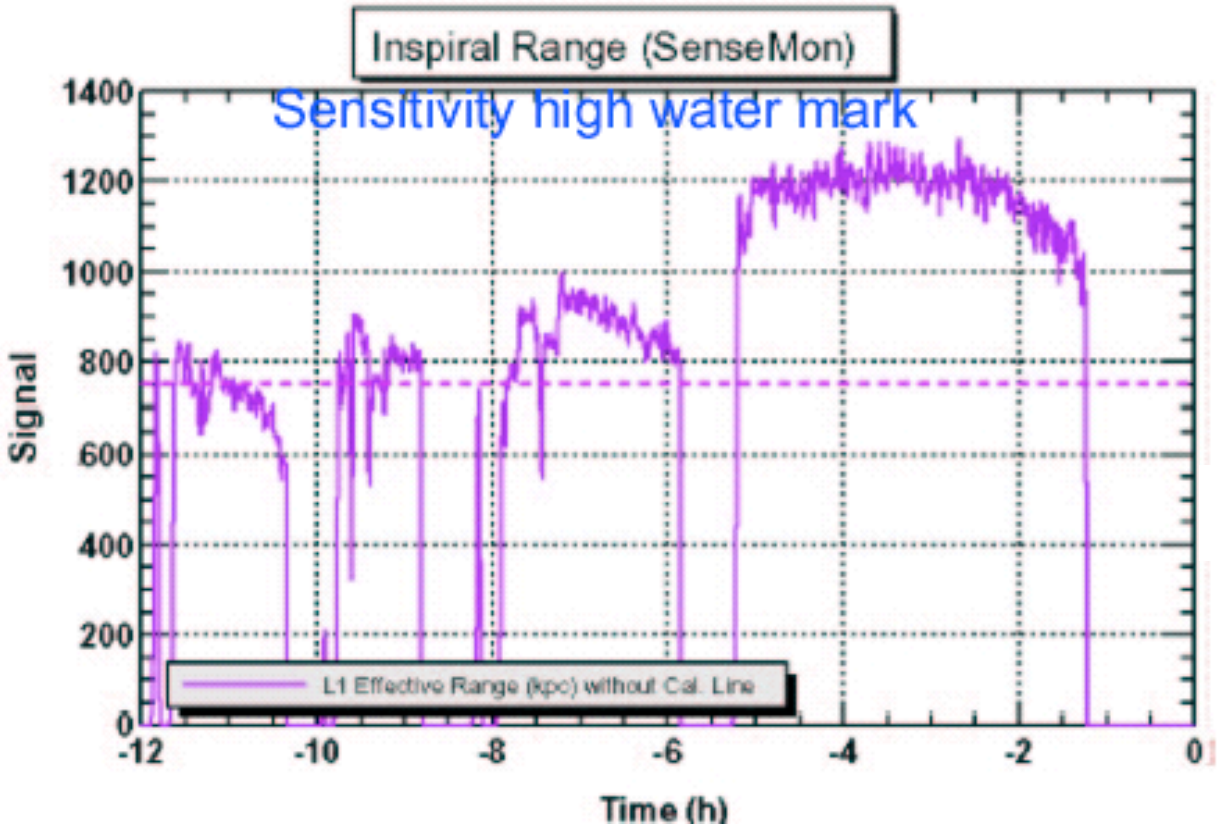

M31 in Andromeda

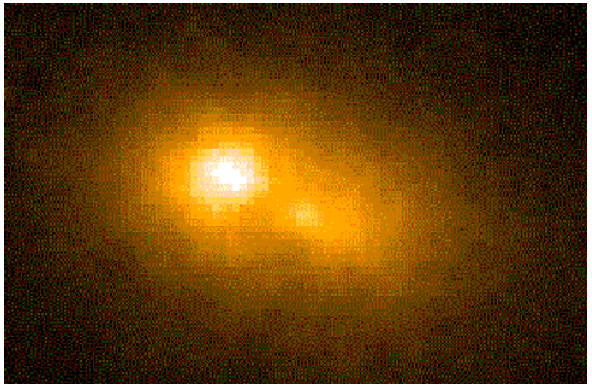

Why will S2,S3 be so much better than S1?

- S2 -- Detector sensitivity
  - » All three detectors showed dramatic improvement over S1 : ~10x
  - » Well matched in sensitivity above ~250 Hz
    - – Better coincidence efficiencies for all sources
    - – Inspiral ranges more well-matched
    - – Stochastic sensitivity scales as $1/(P_1P_2)$
    - – Bursts-- greater ranges
    - – CW sources -- lower h_0
- Data Yield
  - » 4x longer run than S1
    - – All sources will benefit from increased observation time
      - Rate -limited: 1/T
      - Background limited: $1/\sqrt{T}$
    - – Triple coincidence is important for eliminating chance coincidences
  - » S1 required stringent data quality cuts because of nonstationarity
  - » S2 data cuts much less severe
    - – Partial implementation of WFS (wavefront sensing system) for alignment
    - – Better monitoring and greater automation of operational status
    - – Better stationarity for interferometers

S3 -- Detector sensitivity

- » H1, H2 improved at low frequencies to match L1 performance in S2
- » Better matching of sensitivities at low frequencies makes coincidence analysis more effective

Duty cycle

- » Faster lock acquisition due to greater automation
- » Full implementation of WFS at LHO maintains optimum alignment
- » H1, H2 running 70-80% in science mode
- » L1 expected to run about 40% science mode (~ same as S2)

Analysis

- » Greater experience will allow us to exercise and optimize the pipeline as a whole rather than in pieces